

- could be sufficient. Diisopropylaminomethyl polystyrene (Argonaut Technologies) failed to couple with **2a** under the usual conditions.
- [12] All boronic acids used in Table 1 were obtained from commercial sources (Lancaster or Aldrich) except **2h**, which was synthesized according to: H. C. Brown, S. K. Gupta, *J. Am. Chem. Soc.* **1972**, *94*, 4370–4371.
- [13] For an example of the resin capture of diboronic acids using a Suzuki coupling, see S. D. Brown, R. W. Armstrong, *J. Am. Chem. Soc.* **1996**, *118*, 6331–6332.
- [14] M. Vaultier, F. Truchet, B. Carboni, R. W. Hoffmann, I. Denne, *Tetrahedron Lett.* **1987**, *28*, 4169–4172.
- [15] For example, benzenboronic acid is an effective competitive inhibitor of  $\alpha$ -chymotrypsin and subtilisin: M. Philipp, M. L. Bender, *Proc. Natl. Acad. Sci. USA* **1971**, *68*, 478–480.
- [16] For example, see S. Wendeborn, S. Berteina, W. K.-D. Brill, A. De Mesmaeker, *Synlett* **1998**, 671–675.
- [17] Nonoptimized yields of crude isolated compounds of satisfying purity, all characterized by NMR spectroscopy and mass spectrometry.

## Electrochemical Synthesis of $\text{Ba}_2\text{Ag}_8\text{S}_7$ , a Quasi-One-Dimensional Barium Silver(I) Sulfide Containing Mixed $\text{S}^{2-}/\text{S}_2^{2-}$ Ligands\*\*

He Li and Shiou-Jyh Hwu\*

There has been renewed interest in the synthesis of solid-state inorganic materials by means of chemical electrolysis.<sup>[1, 2]</sup> The versatility of the electrochemical technique for exploratory synthesis has been demonstrated by a number of recent reports in materials synthesis.<sup>[2]</sup> Compared to conventional thermal methods, electrochemical synthesis allows greater control over the electronic state of extended solids and possibly structural frameworks as well as product stoichiometry. We have enjoyed numerous successes in the electrochemical crystal growth of copper(I) sulfides in nonaqueous solvents.<sup>[3]</sup> Systematic studies on the electrochemically grown series of compounds  $\text{KCu}_{7-x}\text{S}_4$ , for example, have revealed some unusual stoichiometry-dependent transport anomalies.<sup>[2a, 3]</sup> In light of the fascinating physical properties, we have expanded our search of new coinage metal chalcogenides to include silver. We report here a novel barium silver(I) sulfide obtained in our recent exploratory synthesis of alkaline earth silver(I) sulfides. The  $\text{Ba}_2\text{Ag}_8\text{S}_7$  structure is quasi-one-dimensional and contains mixed  $\text{S}^{2-}$  and  $\text{S}_2^{2-}$  ligands. This discovery provides new insights with respect to possible electrochemical routes for the rational synthesis of inorganic solids.

[\*] Prof. S.-J. Hwu, H. Li  
Department of Chemistry  
Clemson University  
Clemson, SC 29634-0973 (USA)  
Fax: (+1) 864-656-6613  
E-mail: shwu@clemson.edu

[\*\*] Financial support from the Donors of The Petroleum Research Fund, administered by the American Chemical Society, and from, in part, the National Science Foundation (DMR-9612148) is gratefully acknowledged.

Supporting information for this article is available on the WWW under <http://www.wiley-vch.de/home/angewandte/> or from the author.

Prior to this study, all the reported  $\text{A}/\text{Ag}^{\text{I}}/\text{S}$  compounds ( $\text{A}^+$  = alkali metal cation,  $\text{TI}^+$ ,  $\text{NH}_4^+$ ) contained monovalent electropositive cations. A dozen sulfides based on the general formula  $m\text{A}_2\text{S} \cdot n\text{Ag}_2\text{S}$  have been reported thus far. For silver-rich phases ( $m = 1$ ;  $\text{A}_2\text{S} \cdot n\text{Ag}_2\text{S}$ ), there exist  $\text{TI}\text{AgS}$  ( $n = 1$ ),<sup>[4]</sup>  $\text{A}_2\text{Ag}_4\text{S}_3$  ( $\text{A} = \text{K}, \text{Rb}$ ;  $n = 2$ ),<sup>[5]</sup>  $\text{AAg}_3\text{S}_2$  ( $\text{A} = \text{Rb}, \text{Cs}, \text{TI}$ ;  $n = 3$ ),<sup>[6]</sup>  $\text{A}_2\text{Ag}_6\text{S}_4$  ( $\text{A} = \text{Na}, \text{K}$ ;  $n = 3$ ),<sup>[7]</sup>  $\text{AAg}_5\text{S}_3$  ( $\text{A} = \text{K}, \text{Rb}$ ;  $n = 5$ ),<sup>[8]</sup> and  $\text{CsAg}_7\text{S}_4$  ( $n = 7$ ).<sup>[8]</sup> For  $m = 3$ , the only known phase is  $\text{Na}_3\text{AgS}_2$  ( $\equiv 3\text{Na}_2\text{S} \cdot \text{Ag}_2\text{S}$ ).<sup>[9]</sup> In addition,  $\text{TI}\text{Ag}_{5.4}\text{S}_{3.5}$ ,<sup>[10]</sup> a nonstoichiometric compound whose structure has not yet been reported, is known. The compounds listed above were synthesized by high-temperature and/or high-pressure techniques, whereby no compound containing polysulfide has yet been isolated. The silver-based polysulfides known, thus far, are  $[\text{Ag}_2\text{S}_{20}]^{4-}$ ,  $[\text{Ag}(\text{S}_9)]^{1-}$ , and  $[\text{Ag}(\text{S}_5)]^{1-}$ .<sup>[11]</sup> The title compound,  $\text{Ba}_2\text{Ag}_8\text{S}_7$ , was prepared by electrolysis, a method in favor of selective synthesis of low-dimensional conducting solids.<sup>[2a]</sup> It is the first ternary alkaline earth metal silver sulfide known.

Single crystals of  $\text{Ba}_2\text{Ag}_8\text{S}_7$  were grown from a  $\text{BaS}_3$ /ethylenediamine solution in a simple two-electrode chemical cell. The crystal structure was determined by single-crystal X-ray diffraction methods.<sup>[12]</sup> The UV/Vis diffuse reflectance spectrum of  $\text{Ba}_2\text{Ag}_8\text{S}_7$  was taken in the range of 200 nm (6.2 eV) to 2500 nm (0.50 eV).<sup>[13]</sup>

The crystal structural analysis of  $\text{Ba}_2\text{Ag}_8\text{S}_7$  reveals an interesting “stingray” pattern. Figure 1 shows a projected view of the structure where the extended Ag–S framework

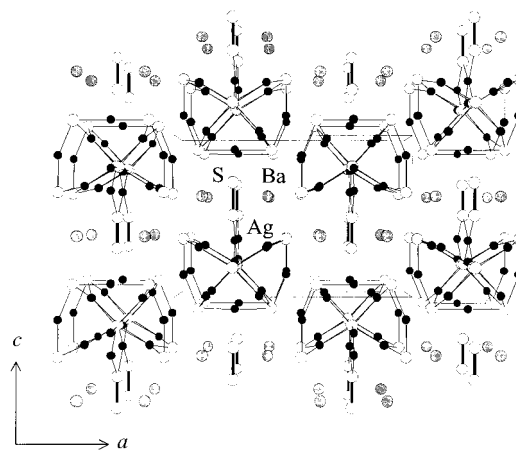


Figure 1. A projected view onto the  $ac$  plane of the  $\text{Ba}_2\text{Ag}_8\text{S}_7$  structure revealing a stingray pattern; see text for details.

exhibits arrays of alternating stingray units. The structure propagates along the  $[100]$  direction with respect to the  $2_1$  screw axis. The parallel arrays of stingray units are stacked head-to-tail in the  $[001]$  direction to create voids where the barium atoms reside.

$\text{Ba}_2\text{Ag}_8\text{S}_7$  adopts a pseudo-one-dimensional structure with respect to the  $\infty[\text{Ag}_8\text{S}_7]$  columns. The projected view of the column resembles the shape of the aforementioned stingray. Figure 2 presents a tilted view showing the coordination environments of the silver atoms. Each column is made of fused  $[\text{Ag}_8\text{S}_5]$  units, each of which is weakly linked to one end of an  $[\text{S}_2]$  unit. The  $[\text{Ag}_8\text{S}_5]$  unit structure consists of a stacked

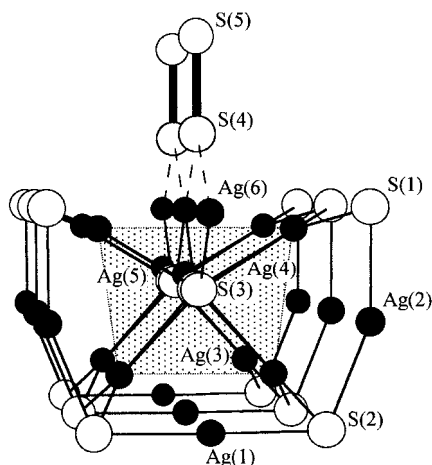


Figure 2. View of the partial structure of a  $[\text{Ag}_8\text{S}_7]$  column consisting of two fused  $[\text{Ag}_8\text{S}_5]$  units; see text for details. A tilted view is shown to discern the coordination environments of the silver atoms. The dashed lines represent the weak linkages between the disulfide units and the "body" of the column. The shaded frame outlines the  $\text{Ag}_4$  core. Selected bond distances [Å]:  $\text{Ag}(1)\text{--S}(2)$  2.450(3) ( $\times 2$ ),  $\text{Ag}(2)\text{--S}(1)$  2.446(3),  $\text{Ag}(2)\text{--S}(2)$  2.498(3),  $\text{Ag}(3)\text{--S}(2)$  2.551(2) ( $\times 2$ ),  $\text{Ag}(3)\text{--S}(3)$  2.567(5) ( $\times 2$ ),  $\text{Ag}(4)\text{--S}(3)$  2.568(4),  $\text{Ag}(4)\text{--S}(3)$  2.569(4),  $\text{Ag}(4)\text{--S}(1)$  2.577(2) ( $\times 2$ ),  $\text{Ag}(5)\text{--S}(3)$  2.581(8) ( $\times 2$ ),  $\text{Ag}(6)\text{--S}(3)$  2.520(9) ( $\times 2$ ),  $\text{Ag}(6)\text{--S}(4)$  2.804(5) ( $\times 2$ ),  $\text{S}(4)\text{--S}(5)$  2.146(6).

C-shaped  $\text{Ag}_3\text{S}_4$  unit ( $\equiv \text{Ag}(1)_{2/2}\text{Ag}(2)_{4/2}\text{S}(1)_{4/2}\text{S}(2)_{4/2}$ ), a distorted square-planar  $\text{Ag}_4$  core ( $\equiv \text{Ag}(3)_{2/1}\text{Ag}(4)_{2/1}$ , indicated by the shaded frame) centered by an  $\text{S-Ag}_x\text{-S}$  unit ( $\equiv \text{Ag}(5)_x\text{S}(3)_{2/2}$ ), and additional  $\text{Ag}(6)_{1-x}$ . The  $\text{Ag}(5)$  and  $\text{Ag}(6)$  sites are partially occupied ( $x = 0.576(7)$ ).<sup>[14]</sup> The latter is 0.11 Å above the center of the edge across two tips ( $2 \times \text{S}(1)$ ) of the  $\text{Ag}_3\text{S}_4$  unit. The planar  $\text{Ag}_4$  core is made of two crystallographically independent silver atoms ( $\text{Ag}(3)$  and  $\text{Ag}(4)$ ).<sup>[12]</sup> The silver atoms adopt three different coordination environments with respect to sulfur atoms: approximately linear coordination for  $\text{Ag}(1)$ ,  $\text{Ag}(2)$ , and  $\text{Ag}(5)$  ( $\angle(\text{S-Ag-S}) = 178.4(2)$ ,  $158.5(1)$ , and  $168.8(4)^\circ$ , respectively), slightly distorted trigonal planar coordination for  $\text{Ag}(3)$  and  $\text{Ag}(4)$  ( $\Sigma(\angle(\text{S-Ag-S})) = 359.6$  and  $358.9^\circ$ , respectively), and distorted square planar coordination for  $\text{Ag}(6)$  ( $\Sigma(\angle(\text{S-Ag-S})) = 360.1^\circ$ ).

The  $[\text{Ag}_8\text{S}_5]$  sulfide unit possesses a reasonably strong covalent framework, judging from the observed  $\text{Ag-S}$  bond distances (2.45–2.58 Å). All the  $\text{Ag-S}$  bond distances are comparable to either 2.43 Å, observed in  $\text{Ag}_2\text{S}$ ,<sup>[15]</sup> or 2.51 Å, the sum of Shannon crystal radii for  $\text{Ag}^+$  (0.81 Å for coordination number 2) and  $\text{S}^{2-}$  (1.70 Å),<sup>[16]</sup> with the exception of the long bond between  $\text{Ag}(6)$  of the  $[\text{Ag}_8\text{S}_5]$  unit and one atom of the  $\text{S}_2^{2-}$  anion (2.80 Å).

The  $[\text{Ag}_8\text{S}_5]$  framework may also possess some bonding interactions between silver(I) cations. It is known that  $d^{10}\text{--}d^{10}$  interactions exist.<sup>[17]</sup> Although the  $\text{Ag-Ag}$  distances are somewhat long (3.26–3.40 Å for the  $\text{Ag}_4$  unit and 2.98–3.19 Å between the  $\text{Ag}_4$  unit and the  $\text{Ag}_3\text{S}_4$  unit) compared to that in  $\text{Ag}$  metal (2.883 Å), there exist possibly weak  $\text{Ag-Ag}$  interactions.

The coexistence of  $\text{S}^{2-}$  and  $\text{S}_2^{2-}$  ligands suggests a possible reductive decomposition reaction with respect to  $\text{BaS}_3$ . Figure 2 shows that the disulfide unit, consisting of atoms

$\text{S}(4)$  and  $\text{S}(5)$ , sits vertically above two adjacent C-shaped units. The observed  $\text{S-S}$  bond distance is 2.146(6) Å, which is comparable to 2.126(9) Å of barium disulfide,  $\text{BaS}_2$ .<sup>[18]</sup> This homonuclear dianion behaves as a ligand to the  $[\text{Ag}_8\text{S}_5]$  unit. We speculate that a partial reduction [Eq. (1)] takes place in the  $\text{BaS}_3$ /ethylenediamine solution. Preliminary studies employing a higher voltage (3 V) result in a pure sulfide phase,  $\text{Ba}_2\text{Ag}_{10}\text{S}_7$ .<sup>[19]</sup> Detailed studies with respect to controlled reduction are underway.



The intercolumn interaction in  $\text{Ba}_2\text{Ag}_8\text{S}_7$  is primarily characterized by the  $\text{Ba-S}$  bonds, and the  $\text{Ba}^{2+}$  cation coordinates to a total of eight sulfur atoms in a bicapped trigonal prism. The  $\text{Ba-S}$  bond distances range from 3.15 to 3.35 Å, which are comparable to 3.26 Å, the sum of the Shannon crystal radii of  $\text{Ba}^{2+}$  (1.56 Å for coordination number 8) and  $\text{S}^{2-}$  (1.70 Å).<sup>[16]</sup> Judging from the long intercolumn  $\text{Ag-S}$  distance (3.184(4) Å), this interaction is too weak to hold the framework together.

The optical spectra reveal that  $\text{Ba}_2\text{Ag}_8\text{S}_7$  is an indirect band-gap semiconductor<sup>[13a]</sup> exhibiting a steep absorption edge. Figure 3 shows the UV/Vis spectrum; the optical band gap

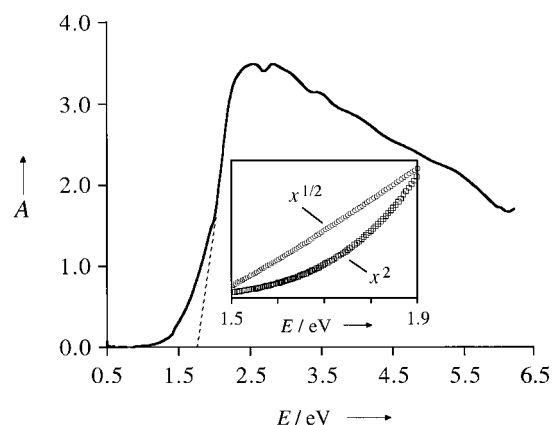


Figure 3. UV/Vis spectrum of  $\text{Ba}_2\text{Ag}_8\text{S}_7$ . Inset: the analyses based on functions  $f(R)^{1/2}$  and  $f(R)^2$ .

obtained by extrapolation of a linear portion of the band edge is about 1.80 eV. Further fitting of the data with  $f(R)^{1/2}$  and  $f(R)^2$  functions confirm that  $\text{Ba}_2\text{Ag}_8\text{S}_7$  is an indirect band-gap semiconductor, as the former gives a linear correlation with energy (see inset of Figure 3). In any event, the observed band gap is consistent with the red-orange color of the compound as well as the experimental observation of the existence of disulfide units. These results lead to an electron-precise formulation,  $(\text{Ba}^{2+})_2(\text{Ag}^+)_8(\text{S}^{2-})_5(\text{S}_2^{2-})$ .

In summary, by employing electrochemical methods, crystals of a novel quasi-one-dimensional barium silver(I) sulfide,  $\text{Ba}_2\text{Ag}_8\text{S}_7$ , have been grown. Upon applying a higher voltage, a new sulfide phase  $\text{Ba}_2\text{Ag}_{10}\text{S}_7$  was synthesized. These preliminary results further illustrate the utility of the electrochemical method for controlled synthesis of reduced polychalcogenide phases. The extended framework exhibits an interesting stingray pattern, and the disulfide unit behaves as a ligand

that governs the packing of the  $^1[\text{Ag}_8\text{S}_5]$  chain. Systematic studies of such materials allow for the possibility of exploiting the redox chemistry of solids containing polychalcogenide  $\text{Q}_x^{2-}$  ligands at the atomic level (e.g., reduction of S–S bonds).

## Experimental Section

**BaS<sub>3</sub>:** A typical batch of BaS<sub>3</sub> was prepared by mixing barium (5.0 g, 36.4 mmol; 99.9%, Strem) and sulfur (3.56 g, 109.2 mmol; 99.99%, Aldrich) in liquid ammonia. The solvated form of barium is  $\text{Ba}^{2+}(2\text{e}^-)(\text{NH}_3)_6^{[19]}$  and gives rise to a dark blue solution. The solution was stirred with a magnetic stirrer and allowed to warm to room temperature over 24 h. A steady flow of dry nitrogen gas was maintained throughout the reaction. The product was obtained as a yellow precipitate, and the powder X-ray diffraction analysis showed that it was amorphous. Heating the amorphous product in a fused silica ampoule at 550 °C under vacuum resulted in mixed crystalline polysulfides—that is, BaS<sub>2</sub> (ca. 70 %) and BaS<sub>3</sub> (ca. 30 %)—according to powder X-ray diffraction.

**Ba<sub>2</sub>Ag<sub>8</sub>S<sub>7</sub>:** Crystals of Ba<sub>2</sub>Ag<sub>8</sub>S<sub>7</sub> were grown in a two-electrode chemical cell. In a typical reaction BaS<sub>3</sub> (0.50 g, used as prepared) was loaded into a 100-mL round-bottom flask in a nitrogen-purged dry box. A rubber septum was used to cap the flask to protect the system from air, and a steady flow of dry nitrogen was maintained throughout the course of the reaction. Ethylenediamine (50 mL; 99 %, Aldrich, distilled over CaH<sub>2</sub>) was injected into the reaction flask. The resulting solution was preheated in a sand bath to 110 °C for 2 h to ensure that all of the electrolytes were dissolved. The reaction temperature was maintained at 110 °C during the course of study. Two parallel electrode plates (1.0 × 1.5 cm<sup>2</sup>) made from silver foil (0.28 mm thick; 99.9 %, Alfa/Aesar) were then immersed in the solution and connected to a constant voltage source. The applied voltage was 1.0 V. The temperature of the electrochemical cell was controlled by a Gemini-2 Temperature Controller (J-KEM Scientific). Crystals of diffraction quality were grown on the anode in about 3 d. The products were dried on a Schlenk line. Two new phases, Ba<sub>2</sub>Ag<sub>8</sub>S<sub>7</sub> (red-orange columns, 95 %) and Ba<sub>2</sub>Ag<sub>10</sub>S<sub>7</sub> (black thin needles, 5 %),<sup>[20]</sup> were identified by single-crystal X-ray diffraction methods.

Received: February 2, 1999 [Z 12985 IE]

German version: *Angew. Chem.* **1999**, *111*, 3253–3256

**Keywords:** barium • electrochemistry • polychalcogenides • silver • solid-state structures • sulfur

- [1] Examples of molten salt electrolysis (MSE) for single-crystal growth of bronzes: a) H. R. Shanks, *J. Cryst. Growth* **1972**, *13/14*, 433–437, and references therein; of LaB<sub>6</sub>; b) I. V. Zubek, R. S. Feigelson, R. A. Huggins, P. A. Pettit, *J. Cryst. Growth* **1976**, *34*, 85–91.
- [2] a) H. Li, R. Mackay, S.-J. Hwu, Y.-K. Kuo, M. J. Skove, Y. Yokota, T. Ohtani, *Chem. Mater.* **1998**, *10*, 3172–3183; b) W. H. McCarroll, K. V. Ramanujachary, M. Greenblatt, F. Cosandey, *J. Solid State Chem.* **1998**, *136*, 322–327; c) A. Nemudry, M. Weiss, I. Gainutdinov, V. Boldyrev, R. Schöllhorn, *Chem. Mater.* **1998**, *10*, 2403–2411; d) X. Wang, L. Liu, R. Bontchev, A. Jacobson, *Chem. Commun.* **1998**, 1009–1010; e) C. J. Warren, R. C. Haushalter, A. B. Bocarsly, *J. Alloys Compd.* **1995**, *229*, 175–205; f) L. Z. Zhao, *Solid State Commun.* **1995**, *94*, 857–859; g) G. L. Roberts, S. M. Kauzlarich, R. S. Glass, J. C. Estill, *Chem. Mater.* **1993**, *5*, 1645–1650; h) T. N. Nguyen, D. M. Giaquinta, W. M. Davis, H. C. zur Loye, *Chem. Mater.* **1993**, *5*, 1273–1276; i) V. C. Korthius, R. D. Hoffman, A. W. Sleight, *Mater. Res. Bull.* **1992**, *27*, 1379–1384; j) M. L. Norton, H. Y. Tang, *Chem. Mater.* **1991**, *3*, 431–434; k) M. D. Ward in *Electroanalytical Chemistry, A Series of Advances* (Ed.: A. J. Bard), Marcel Dekker, New York, **1989**, pp. 181–312, and references therein.
- [3] a) S.-J. Hwu, H. Li, R. Mackay, Y.-K. Kuo, M. J. Skove, M. Mahapatro, C. K. Bucher, J. P. Halladay, M. W. Hayes, *Chem. Mater.* **1998**, *10*, 6–9; b) Y.-K. Kuo, M. J. Skove, D. T. Verebelyi, H. Li, R. Mackay, S.-J. Hwu, M.-H. Whangbo, J. W. Brill, *Phys. Rev. B* **1998**, *57*, 3315–3325; c) K.-S. Lee, D.-K. Seo, M.-H. Whangbo, H. Li, R. Mackay, S.-J. Hwu, *J. Solid State Chem.* **1997**, *134*, 5–9.
- [4] a) J. C. Tedennac, B. Gardes, G. Burn, E. Philippot, M. Maurin, *J. Solid State Chem.* **1980**, *33*, 429–433; b) K. Klepp, *Monatsh. Chem.* **1980**, *111*, 1433–1436.
- [5] W. Bronger, C. Burschka, *Z. Anorg. Allg. Chem.* **1976**, *425*, 109–116.
- [6] a) C. Burschka, W. Bronger, *Z. Anorg. Allg. Chem.* **1977**, *430*, 61–65; b) K. O. Klepp, *J. Less-Common Met.* **1985**, *107*, 139–146.
- [7] P. T. Wood, W. T. Pennington, J. W. Kolis, *J. Chem. Soc. Chem. Commun.* **1993**, 235–236.
- [8] a) M. Emirdag, G. L. Schimek, J. W. Kolis, *Acta Crystallogr. Sect. C* **1998**, *54*, 1376–1378; b) P. T. Wood, W. T. Pennington, J. W. Kolis, *Inorg. Chem.* **1994**, *33*, 1556–1558; c) J. Huster, *J. Alloys Compd.* **1992**, *183*, 377–384.
- [9] K. O. Klepp, W. Bronger, *J. Less-Common Met.* **1985**, *106*, 91–101.
- [10] K. O. Klepp, *Z. Kristallogr.* **1983**, *162*, 136.
- [11] a) A. Mueller, M. Roemer, H. Boegge, E. Krickemeyer, F. W. Baumann, K. Schmitz, *Inorg. Chim. Acta* **1984**, *89*(1), L7–L8; b) A. Mueller, J. Schimanski, M. Roemer, H. Boegge, F. W. Baumann, W. Eltzner, E. Krickemeyer, U. Billerbeck, *Chimia* **1985**, *39*(1), 25–27; c) R. M. Herath Banda, D. C. Craig, I. G. Dance, M. L. Scudder, *Polyhedron* **1989**, *8*, 2379–2383.
- [12] a) Crystal data of Ba<sub>2</sub>Ag<sub>8</sub>S<sub>7</sub>: red-orange column crystal (0.05 × 0.05 × 0.3 mm<sup>3</sup>), *M<sub>r</sub>* = 1363.8, orthorhombic, space group *Pmmn* (no. 59), *a* = 15.643(3), *b* = 4.407(2), *c* = 10.869(2) Å, *V* = 749.3(4) Å<sup>3</sup>, *Z* = 2,  $\rho_{\text{calcd}}$  = 6.044 g cm<sup>−3</sup>,  $\mu$  = 163.29 cm<sup>−1</sup>. Data collection: Nicolet R3mV diffractometer,  $\omega$  mode, MoK $\alpha$  radiation ( $\lambda$  = 0.71073 Å), *T* = 295 K. Of 1014 unique reflections measured, 851 (*F* > 6 $\sigma$ (*F*)) were used for the calculation. Lorentz-polarization and empirical absorption corrections based on three azimuthal scans (2 $\theta$  = 14.43°, 19.31°, 23.93°) were applied to the intensity data (transmission factors: 0.5892–0.7068). The TEXSAN software package<sup>[12c,d]</sup> was used for crystal structure solution and refinement. The atomic coordinates of fully occupied atoms were determined using the SHELXS-86 program.<sup>[12e]</sup> Those of disordered S and partially occupied Ag atoms were resolved using a difference Fourier map with the SHELXS-93 program.<sup>[12f]</sup> Final *R* = 0.034, *R<sub>w</sub>* = 0.055, GOF = 1.44 for 65 parameters; min./max. residual electron density −4.69/ +3.65 e Å<sup>−3</sup>; b) Further details of the crystal structure investigation may be obtained from the Fachinformationszentrum Karlsruhe, D-76344 Eggenstein-Leopoldshafen, Germany (fax: (+49) 7247-808-666; e-mail: crysdata@fiz-karlsruhe.de) on quoting the depository number CSD-410642; c) TEXSAN: Single Crystal Structure Analysis Software, Version 1.6b, Molecular Structure Corp., The Woodlands, TX, **1993**; d) “Scattering Factors for Non-hydrogen Atoms”: D. T. Cromer, J. T. Waber, *International Tables for X-ray Crystallography, Vol. IV*, Kynoch, Birmingham, UK, **1974**, Table 22A, pp. 71–98; e) G. M. Sheldrick in *Crystallographic Computing 3* (Eds.: G. M. Sheldrick, C. Krüger, R. Goddard), Oxford University Press, London, **1985**, pp. 175–189; f) G. M. Sheldrick, SHELXS-93, Göttingen, Germany, **1993**.
- [13] Optical absorption spectra were obtained from a PC-controlled SHIMADZU UV-3100 UV/vis/near-IR spectrometer equipped with an integrating sphere (standard equipment for diffuse reflectance). BaSO<sub>4</sub> was used as a reflectance standard. Data were collected in the reflectance mode (*R* [%]) and manually converted into arbitrary absorption units (*a/s*) (*a*: absorption coefficient, *s*: scattering coefficient) with Equation (2): a) J. I. Pankove, *Optical Processes in Semiconductors*, Dover Publications, New York, **1971**, pp. 34–42; b) P. Kubelka, F. Z. Munk, *Tech. Phys. USSR* **1931**, *12*, 593; c) P. Kubelka, *J. Opt. Soc. Am.* **1948**, *38*, 448–457.

$$A = f(R) = a/s = (1 - R)^2/2R \quad (2)$$

- [14] The atoms Ag(5) and Ag(6) were first refined independently to result in values of 0.58(1) and 0.431(9), respectively, which are summed together nearly to one. These two atoms were then refined with a constrained total occupancy of one to give the value of *x* denoted in the formula (0.576(7)).
- [15] R. J. Cava, F. Reidinger, B. J. Wuensch, *J. Solid State Chem.* **1980**, *31*, 69–80.
- [16] R. D. Shannon, *Acta Crystallogr. Sect. A* **1976**, *32*, 751–767.

- [17] M. Jansen, *Angew. Chem.* **1987**, *99*, 1136–1148; *Angew. Chem. Int. Ed. Engl.* **1987**, *26*, 1098–1110.  
 [18] a) H. G. von Schnering, N.-K. Goh, *Naturwissenschaften* **1974**, *61*, 272; b) I. Kawada, K. Kato, S. Yamaoka, *Acta Crystallogr. Sect. B* **1975**, *31*, 2905–2906.  
 [19] a) W. E. Ferneliuss, G. W. Watt, *Chem. Rev.* **1937**, *20*, 195–258; b) Mentrel, *Bull. Soc. Chim.* **1903**, *29*, 493–503; c) S. Yamaoka, J. T. Lemley, J. M. Jenks, H. Steinfink, *Inorg. Chem.* **1975**, *14*, 129–131.  
 [20] Crystal data of  $\text{Ba}_2\text{Ag}_{10}\text{S}_7$ : black needle crystal, monoclinic, space group  $C2/m$  (no. 12),  $a = 14.460(3)$ ,  $b = 4.295(2)$ ,  $c = 13.467(3)$  Å,  $\beta = 103.88(3)^\circ$ ,  $V = 812.1(5)$  Å<sup>3</sup>,  $Z = 2$ .

## NMR Spectroscopic Structural Determination of Organozinc Reagents: Evidence for “Highly Coordinated” Zincates\*\*

T. Andrew Mobley and Stefan Berger\*

In an interesting series of papers from the laboratories of Uchiyama and Sakamoto,<sup>[1]</sup> differences in the reactivity between stoichiometrically formulated  $[\text{Me}_3\text{Zn}]\text{Li}$  and  $[\text{Me}_4\text{Zn}]\text{Li}_2$  led the authors to postulate the existence of a tetracoordinated zinc complex in solution.  $^1\text{H}$  NMR studies indicate that only one type of methyl resonance exists in these species, even at very low temperatures. However, as noted by the authors the NMR spectra observed could be the result of a rapid equilibrium of different complexes. Based upon our recent success in using fully  $^{13}\text{C}$ -labeled material to identify the number of methyl groups bound to the central copper atom in analogous cuprate complexes,<sup>[2]</sup> we undertook a structural investigation of the above mentioned organozincates.

The use of fully  $^{13}\text{C}$ -labeled material results, in the absence of  $^1\text{H}$ -decoupling irradiation, in magnetic inequivalence of chemically equivalent carbon atoms. This result is a consequence of the difference in the  $\text{C}_\text{H}$  coupling between a carbon atom and those protons directly attached and those protons attached to another  $^{13}\text{C}$ -labeled methyl group in the same molecule. Since the magnetic inequivalence of the carbon atoms allows the observation of the carbon–carbon coupling constant over two bonds, analysis of the spectra provides an easy method of counting the number of labeled methyl groups attached to the metal center.

As a base compound, the neutral  $(^{13}\text{CH}_3)_2\text{Zn}$  species (**1**) was synthesized by heating  $^{13}\text{CH}_3\text{I}$  and Zn powder in the presence of a small amount of Cu catalyst in a sealed glass system.<sup>[3]</sup>

Vacuum transfer of the volatile material from the solid residue to a liquid-nitrogen cooled flask resulted in the isolation of **1** contaminated by a small amount of  $^{13}\text{CH}_3\text{I}$  starting material. A small amount of **1** was dissolved in  $[\text{D}_8]\text{THF}$  or  $[\text{D}_{14}]\text{hexane}$  and the  $^1\text{H}$  and  $^1\text{H}$ -coupled  $^{13}\text{C}$  NMR spectra were obtained at 400 and 600 MHz, respectively. Expansions of the methyl regions of the  $^{13}\text{C}$  NMR spectra are shown for **1** in hexane and **1** in  $[\text{D}_8]\text{THF}$  (Figure 1a and 1b, respectively). For compar-

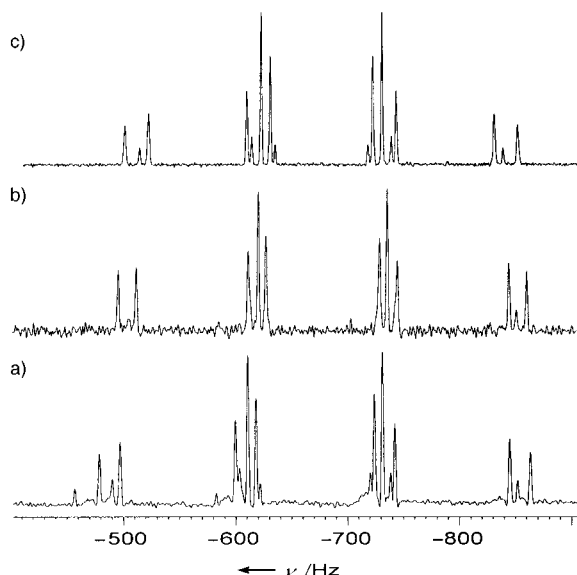


Figure 1.  $^1\text{H}$  coupled  $^{13}\text{C}$  NMR spectra at  $-80^\circ\text{C}$ : a) **1** (0.08 M) in hexane; b) **1** (0.35 M) in  $[\text{D}_8]\text{THF}$ ; c) **2** (0.26 M) in  $[\text{D}_8]\text{THF}$ .

ison the spectrum of the analogous compound  $[(^{13}\text{CH}_3)_2\text{Cu}]\text{Li}$  (**2**) in  $[\text{D}_8]\text{THF}$  is also shown (Figure 1c). All three spectra show a similar coupling pattern with only slight changes in the coupling constants. The spectra were modeled on the basis of the higher-order coupling pattern of an  $\text{A}_3\text{XX}'\text{A}_3'$  system and the calculated coupling constants are summarized in Table 1. Dimethylzinc synthesized by treatment of  $\text{ZnI}_2$  with two equivalents of  $^{13}\text{CH}_3\text{Li}$  resulted in identical spectra when the concentration of the zinc species was low.

The species  $[(^{13}\text{CH}_3)_3\text{Zn}]\text{Li}$  (**3**) could be synthesized by treatment of  $(^{13}\text{CH}_3)_2\text{Zn}$  with one equivalent of  $^{13}\text{CH}_3\text{Li}$ . In practice a suitable excess of  $^{13}\text{CH}_3\text{Li}$  was used to account for the presence of the  $^{13}\text{CH}_3\text{I}$  contaminant. The  $^1\text{H}$  and  $^{13}\text{C}$  NMR spectra of this sample also show a higher order coupling pattern; however, the coupling pattern differs substantially from that of dimethylzinc (Figure 2a). These spectra could be modeled successfully with a  $\text{A}_3\text{XA}_3'\text{X}'\text{A}_3''\text{X}''$  system (Figure 3).<sup>[4]</sup> The resulting calculated spectrum is shown for comparison in Figure 2b and the calculated coupling constants are summarized in Table 1.

Addition of one additional equivalent of  $^{13}\text{CH}_3\text{Li}$  results in the formation of  $[(^{13}\text{CH}_3)_4\text{Zn}]\text{Li}_2$  (**4**). The  $^1\text{H}$  and  $^{13}\text{C}$  spectra indicate that the bulk of the zinc-containing material is identical to **3**. However, in addition to one equivalent of  $^{13}\text{CH}_3\text{Li}$  in its tetrahedral tetrameric form, a broad, weak resonance is observed at  $\delta = -12$  (Figure 4). Furthermore, after an overnight  $^{13}\text{C}$  NMR acquisition at high field

[\*] Prof. Dr. S. Berger, Dr. T. A. Mobley  
 Institut für Analytische Chemie  
 Fakultät für Chemie und Mineralogie der Universität  
 Linnéstrasse 3, D-04103 Leipzig (Germany)  
 Fax: (+49) 341-9736115  
 E-mail: stberger@rz.uni-leipzig.de

[\*\*] This work was supported by the Fonds der Chemischen Industrie.